ORIGINAL RESEARCH PAPER

Cross-linked sulfonated polyacrylamide (Cross-PAA-SO$_3$H) attached to nano-Fe$_3$O$_4$ as a superior catalyst for the synthesis of oxindoles

Hossein Shahbazi-Alavi[1,], Javad Safaei-Ghomi [2]*

[1] *Young Researchers and Elite Club, Kashan Branch, Islamic Azad University, Kashan, Iran*
[2] *Department of Organic Chemistry, Faculty of Chemistry, University of Kashan, Iran*

ABSTRACT

Cross-linked sulfonated polyacrylamide (Cross-PAA-SO$_3$H) attached to nano-Fe$_3$O$_4$ as an efficient heterogeneous solid acid catalyst has been used for the preparation of spiro[pyrazoloquinoline-oxindoles] and spiro[chromenopyrazolo-oxindoles] through a four-component reactions of phenylhydrazine or hydrazine hydrate, isatins, ketoesters and naphthylamine or 2-naphthol under reflux conditions in ethanol. The remarkable advantages of this methodology are easy work-up, short reaction times, high to excellent product yields, operational simplicity, low catalyst loading and reusability of the catalyst.

Keywords: *Isatin; Nanocatalyst; Nano-Fe$_3$O$_4$, Oxindoles; Polyacrylamide*
© 2019 Published by Journal of Nanoanalysis.

INRODUCTION

Spirooxindoles have appeared as a series of significant heterocycles due to their presence in a wide spectrum of natural and synthetic organic compounds [1-3], with various biological characterizes including antimicrobial [4-6], antitumor [7-8], antidiabetic [9], and can also serve as synthetic intermediates for diverse kinds of pharmaceuticals or drug precursors [10]. These activities make spirooxindoles attractive goals in organic synthesis. The synthesis of spirooxindoles has been reported using *p*TSA [11,12], piperidine [13], alum (KAl(SO$_4$)$_2$. 12H$_2$O) [14], SBA-Pr-NH$_2$ [15], nanocrystalline MgO [16], and *L*-Proline [17]. However, some of the developed methods endure drawbacks such as long reaction times and harsh reaction conditions. To elude these restrictions, discovery of an efficient, easily accessible catalyst with high catalytic activity for the preparation of spirooxindoles is still favored. The modifying cross-linked polyacrylamides make them attractive objects in chemistry and polymer science [18-20]. Sulfonated polyacrylamides have unique characteristics such as high strength, hydrophilicity, and proton conductivity [21-22]. Recently, magnetic nanoparticles (MNPs) have been successfully utilized to immobilize enzymes, polymers, transition metal catalysts and organocatalysts [23-24]. In the current study, we investigated an easy and rapid method for the synthesis of spiro[pyrazoloquinoline-oxindoles] and spiro[chromenopyrazolo-oxindoles] through a four-component reactions of phenylhydrazine or hydrazine hydrate, isatins, ketoesters and naphthylamine or 2-naphthol using cross-linked sulfonated polyacrylamide (Cross-PAA-SO$_3$H), attached to nano-Fe$_3$O$_4$, as an efficient catalyst under reflux conditions in ethanol (Scheme 1).

EXPERIMENTAL SECTION

Chemicals and apparatus

NMR spectra were obtained on a Bruker Avance 400 MHz spectrometer (^{1}H NMR at 400 Hz, ^{13}C NMR at 100 Hz) in DMSO-*d$_6$* using TMS

* Corresponding Author Email: *hossien_shahbazi@yahoo.com*
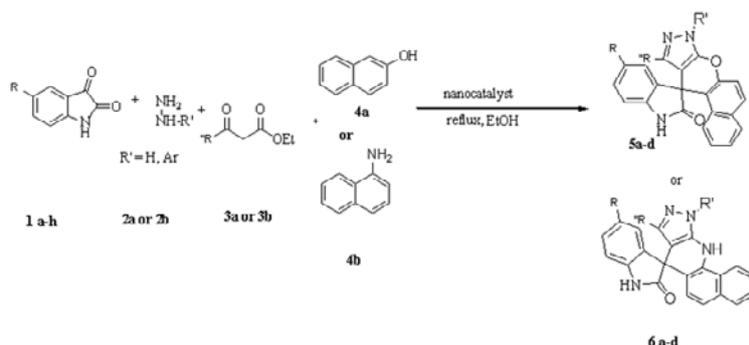
Scheme 1. Synthesis of spiro-oxindoles

as an internal standard. Powder X-ray diffraction (XRD) was carried out on a Philips diffractometer of X'pert Company with monochromatized Cu Kα radiation (λ = 1.5406 Å). Microscopic morphology of products was visualized by SEM (MIRA3). The thermogravimetric analysis (TGA) curves are recorded using a V5.1A DUPONT 2000. The magnetic measurement of samples were carried out in a vibrating sample magnetometer (VSM) (Meghnatis Daghigh Kavir Co.; Kashan Kavir; Iran) at room temperature in an applied magnetic field sweeping between ±10 k Oe.

Preparation of Crosslinked Sulfonated Polyacrylamide (Cross-PAA-SO₃H):

In a round-bottom flask (200 mL) equipped with magnetic stirrer and condenser, 5 g of acrylamid (AAM) (70 mmol) and 5.17 g of 2-acryloylamino-2-methylpropane-1-sulfonic acid (25 mmol) (AAMPS), (approximately AAM/AAMPS (3/1)) and 0.77 gr of N,N-methylene-bis-acrylamid (NNMBA) (5 mmol) as crosslinking agent and benzoyl peroxide as initiator were added to 80 mL EtOH under reflux condition for 5 h. After completion of the reaction, the white precipitate was formed, filtered, washed and dried in vacuum oven in 70 ℃ for 12 h. The weight of polymer was 10.1 gr with the yield of 91.8 %. This catalyst was characterized with infrared spectroscopy and back titration acid-base to confirm sulfonation and determine accurate sulfonation levels. Acidic capacity of this catalyst was estimated 1.1 mmol/g.

Preparation of cross-linked solfonated polyacrylamide@nano-Fe₃O₄:

1g of cross-linked sulfonated polyacrylamide was poured in 100 mL round bottom flask under stirring at room temperature, and then 50 mL HCl (0.4 M) was added to flask. 0.43 g FeCl₂.4H₂O and

1.17 g FeCl₃.6H₂O were added to the mixture. The mixture was stirred until dissolved completely (flask 1). In another 500 mL round-bottom flask 2, 400 mL aqueous solution of NH₃ (0.7M) was poured under argon gas. Then flask 1 was added to flask 2 immediately. Nanocatalyst was filtered and washed with water (2×25 mL) and dried in oven on 50 ℃ C.

General procedure for the synthesis of spirooxindoles:

A mixture of isatin derivatives (1 mmol), phenylhydrazine or hydrazine hydrate (1 mmol), alkyl acetoacetate (1 mmol), naphthalene amine or 2-naphthol (1 mmol) and Cross-PAA-SO₃H@ nano-Fe₃O₄ (7 mg) in EtOH (15 mL) was refluxed for the appropriate times. The reaction was monitored by TLC (*n*-hexan/ethyl acetate 8:2). After completion of the reaction, the mixture was cooled to room temperature and the nanocatalyst was easily separated using an external magnet. The solvent was evaporated and the obtained solid was filtered and then washed with EtOH and water to get pure product.

Spectral data

5'-Chloro-10-methyl-8H-spiro [benzo-[5, 6]-chromeno-[2, 3-c]-pyrazole-11, 3'-indolin]-2'-one (5a): Yellow solid; M. p. 196-198 °C, – IR (KBr): ν = 3321, 3201, 3071, 1689, 1618, 1433 cm⁻¹. – ¹H NMR (400 MHz, DMSO-d₆): δ (ppm) = 1.86 (s, 3H, CH₃), 6.90-6.95 (m, 2H, ArH), 7.10-7.15 (m, 6 H, ArH), 7.70 (s, 1H, ArH), 10.24 (s, 1H, NH-CO), 11.25 (s, 1H, NH). – ¹³C NMR (100 MHz, DMSO-d₆): δ (ppm) = 10.13 (CH₃), 48.80 (C), 108.70 (C), 111.09 (C), 117.51 (CH), 120.28 (2CH), 123.20 (CH) 124.51 (C), 125.90 (2CH), 125.99 (2C), 128.35 (C), 130.74 (CH), 133.93 (C-Cl), 133.98 (C), 136.70 (CH), 137.92 (C), 142.56 (CH-C-Cl), 156.70 (CH-C-O), 163.74 (C=O).– Analysis for C₂₂H₁₄ClN₃O₂:

calcd. C 68.13, H 3.64, N 10.83; Found C 68.06; H 3.55, N, 10.70.

10-Methyl-8H-spiro [benzo-[5,6]-chromeno-[2, 3-c]-pyrazole-11, 3'-indolin]-2'-one (5b): Yellow solid; M. p. 185-187 °C, – IR (KBr): ν = 3332, 3202, 3071, 1680, 1616, 1435 cm^{-1} . – ^{1}H NMR (400 MHz, DMSO-d$_6$): δ (ppm) = 1.92 (s, 3H, CH$_3$), 6.45 (m, 2H, ArH), 6.75 (m, 2H, ArH), 6.86 (m, 2H, ArH), 6.96-7.21 (m, 4H, ArH), 10.18 (s, 1H, NH-CO), 11.20 (s, 1H, NH). – ^{13}C NMR (100 MHz, DMSO-d$_6$): δ (ppm) = 10.10 (CH$_3$), 49.07 (C), 106.72 (C), 111.07 (C), 112.09 (CH), 117.34 (2CH), 120.13 (CH), 123.20 (2CH), 124.37 (CH), 125.99 (CH), 126.90 (CH), 128.63 (C), 128.82 (CH), 130.66 (C), 133.92 (C) , 135.90 (C), 137.00 (C), 141.33 (C), 156.60 (CH-C-O), 165.07 (C=O).– Analysis for C$_{22}$H$_{15}$N$_3$O$_2$: calcd. C 74.78, H 4.28, N 11.89; Found C 74.65, H 4.22, N 11.74.

5'-Methyl-10-methyl-8H-spiro [benzo-[5, 6]-chromeno-[2, 3-c]-pyrazole-11, 3'-indolin]-2'-one (5c): Yellow solid; M. p. 171-173 °C, – IR (KBr): ν = 3330, 3209, 3075, 1682, 1613, 1433 cm^{-1}. – ^{1}H NMR (400 MHz, DMSO-d$_6$): δ (ppm) = 1.90 (s, 3H, CH$_3$), 2.30 (s, 3H, CH$_3$), 6.50-6.80 (m, 4H, ArH), 6.82-6.87 (m, 2H, ArH), 7.16-7.35 (m, 3H, ArH), 10.18 (s, 1H, NH-CO), 11.20 (s, 1H, NH). – ^{13}C NMR (100 MHz, DMSO-d$_6$): δ (ppm) = 10.19 (CH$_3$), 23.45 (CH$_3$), 49.10 (C), 107.75 (C), 112.04 (C), 112.18 (CH), 117.44 (2CH), 120.22 (CH), 123.25 (2 CH), 124.41 (C), 125.90 (C), 126.84 (CH), 128.74 (CH), 128.84 (C), 130.72 (CH), 133.94 (C), 135.96 (C), 137.21 (C), 141.43 (C), 156.64 (CH-C-O), 165.12 (C=O).– Analysis for C$_{23}$H$_{17}$N$_3$O$_2$: calcd. C 75.19, H 4.66, N 11.44; Found C 75.25, H 4.55, N 11.42.

5'-nitro-10-Methyl-8H-spiro [benzo-[5, 6]-chromeno-[2, 3-c]-pyrazole-11, 3'-indolin]-2'-one (5d): yellow solid; M. p. 190-192 °C, – IR (KBr): ν = 3335, 3223, 3087, 1692, 1627, 1430 cm^{-1}, – ^{1}H NMR (400 MHz, DMSO-d$_6$): δ (ppm) = 1.88 (s, 3H, CH$_3$), 6.92-6.98 (m, 2H, ArH), 7.14-7.18 (m, 6H, ArH), 7.92 (s, 1H, ArH), 10.24 (s, 1H, NH-CO), 11.25 (s, 1H, NH).– ^{13}C NMR (100 MHz, DMSO-d$_6$): δ (ppm) = 10.18 (CH$_3$), 48.78 (C), 107.78 (C) , 111.29 (C), 117.63 (2CH), 120.38 (CH), 124.22 (2CH), 124.55 (CH), 125.93 (C), 126.80 (CH), 128.10 (CH), 128.25 (CH) , 130.87 (C), 133.76 (C), 134.57 (C), 137.88 (C), 139.62 (C), 143.42 (C-NO$_2$), 156.62 (CH-C-O),, 163.95 (C=O).– Analysis for C$_{22}$H$_{14}$N$_4$O$_4$: calcd. C 66.33, H 3.54, N 14.06; Found C 66.22, H 3.41, N 14.10.

RESULTS AND DISCUSSION

Characterization of the nanocatalyst

In this study, we synthesized the cross-linked sulfonated polyacrylamide (Cross-PAA-SO$_3$H) with simultaneous radical co-polymerization in presence of initiator and crosslinking agent. The FT-IR absorbance spectra of the dried cross-linked sulfonated polyacrylamide (poly AAM-*co*-AAMPS), Fe$_3$O$_4$ and Cross-PAA-SO$_3$H@nano-Fe$_3$O$_4$ are shown in Fig. 1. The N–H stretching vibration of the amide groups in AAm and AAMPS and overlapping O–H stretching vibration of sulfonic acid group in AAMPS are observed in the region 3100–3500 cm^{-1}. The strong absorption band in 1658 cm^{-1} can be attributed to the stretching vibrations of C=O groups in both AAm and AAMPS. Secondary amide band of AAMPS unit has a peak in 1545 cm^{-1}. The sharp peak at
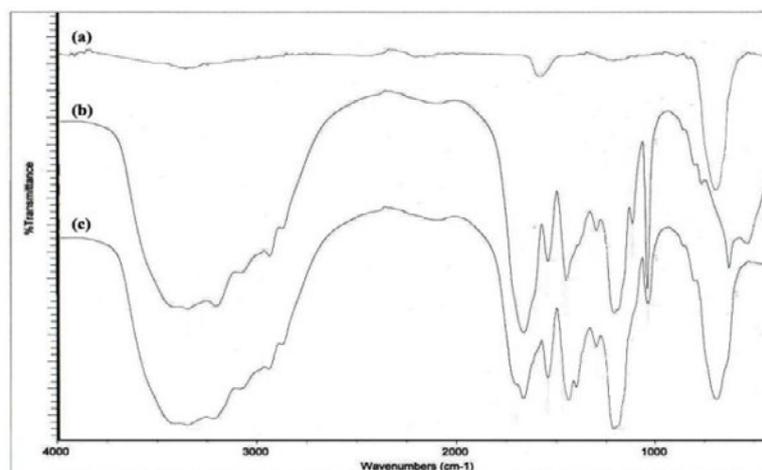

Fig. 1. The FT-IR spectra of (a) Fe$_3$O$_4$ NPs, (b) Cross-PAA-SO$_3$H and (c) Cross-PAA-SO$_3$H@ nano-Fe$_3$O$_4$

1042 cm $^{-1}$ is related to sulfonic acid (–SO$_3$H) group. The symmetric band of SO$_2$ is observed in the 1178-1216 cm $^{-1}$. The band at 1453 cm^{-1} is assigned to the stretching vibration of the C–N bond (amide) and the asymmetric bending of the C–H bond in methyl groups of AMPS. Table 1 gives the main characteristic peak assignment of the FT-IR spectra. Also a schematic illustration of the reaction is shown in the scheme 2. The absence of the olefinic band at 1620–1635 cm $^{-1}$ confirms that, there is no residual monomer in the system. The results in Fig. 1 (c) suggest the integration of Fe$_3$O$_4$ NPs and Cross-PAA-SO$_3$H.

The particle size and morphology of Cross-PAA-SO$_3$H@nano-Fe$_3$O$_4$ was determined by Scanning Electronic Microscopy (SEM). The statistic of results from SEM images clearly demonstrate that the average size of Cross-PAA-SO$_3$H@nano-Fe$_3$O$_4$ is about 7-25 nanometers (Fig. 2).

Fig. 3 shows the powder X-ray diffraction (XRD) pattern. The pattern agrees well with the reported pattern for Fe$_3$O$_4$ (JCPDS No. 75-0449). The crystallite size of Cross-PAA-SO$_3$H@nano-Fe$_3$O$_4$ calculated by the Debye–Scherer equation is

about 20-25 nm, in good agreement with the result obtained by SEM.

An EDS (energy dispersive X-ray) spectrum of Cross-PAA-SO$_3$H@nano-Fe$_3$O$_4$ (Fig. 4) shows that the elemental compositions are carbon, oxygen, sulfur, iron and nitrogen.

The magnetic properties of nano-Fe$_3$O$_4$ and Cross-PAA-SO$_3$H@nano-Fe$_3$O$_4$ were determined with the help of a vibrating sample magnetometer (VSM) at room temperature in an applied magnetic field sweeping between ±10,000 Oe (Fig. 5). The amount of saturation-magnetization for nano-Fe$_3$O$_4$ and Cross-PAA-SO$_3$H@nano-Fe$_3$O$_4$ is 47.2 emu/g and 26.8 emu/g.

Thermogravimetric analysis (TGA) evaluates the thermal stability of the Cross- PAA-SO$_3$H@ nano-Fe$_3$O$_4$. These nanoparticles show suitable thermal stability without a significant decrease in weight (Fig. 6). The weight loss at temperatures below 200 ºC is due to the removal of physically adsorbed solvent and surface hydroxyl groups. The curve shows a weight loss about 20 % from 250 to 600 ºC, resulting from the decomposition of the organic spacer grafting to the nano-Fe$_3$O$_4$ surface.

Table 1: Peak assignment of crosslinked Sulfonated Polyacrylamide (Cross-PAA-SO$_3$H)

Peak position (cm^{-1})	Assignment
3100-3500	N-H stretching of NH$_2$,OH stretching of (- SO$_3$H)
1658	C=O stretching of CO in AAM and AAMPS
1545	Secondary amid band of AAMPS
1042	Sulfonic acid (- SO$_3$H) group
1175-1216	Symmetric band of SO$_2$
1453	Stretching of the C-N band (amid)
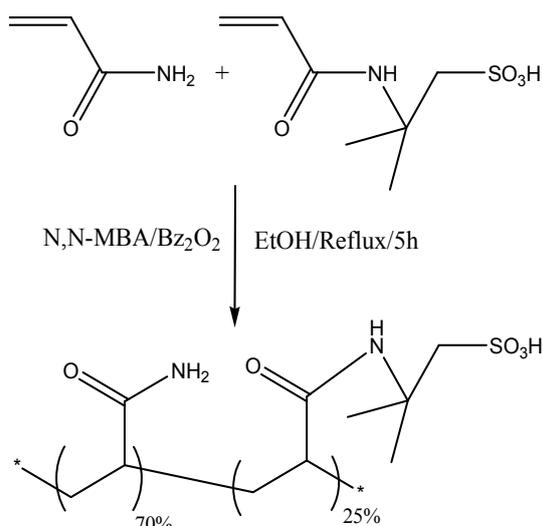
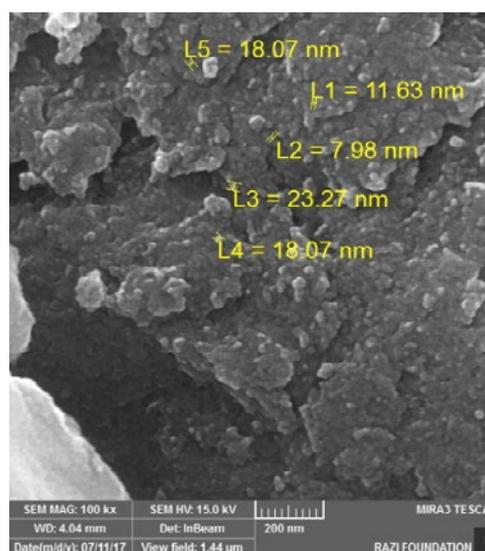Scheme 2. Preparation of cross-linked Sulfonated Polyacrylamide (Cross-PAA-SO$_3$H)

Fig. 2. SEM image of Cross-PAA-SO$_3$H@nano-Fe$_3$O$_4$

Catalytic behaviors of Cross-PAA-SO$_3$H@nano-Fe$_3$O$_4$ for the synthesis of oxindoles

Initially, we had optimized various reaction parameters for the synthesis of spirooxindoles by the condensation reaction of 5-chloro-isatin, hydrazine hydrate, ethyl acetoacetate and 2-naphthol as a model reaction. The model reactions were performed by CAN, NaHSO$_4$, Et$_3$N, NiCl$_2$, ZrOCl$_2$, *p*-TSA and nano-Fe$_3$O$_4$ and Cross-PAA-SO$_3$H@nano-Fe$_3$O$_4$. Several
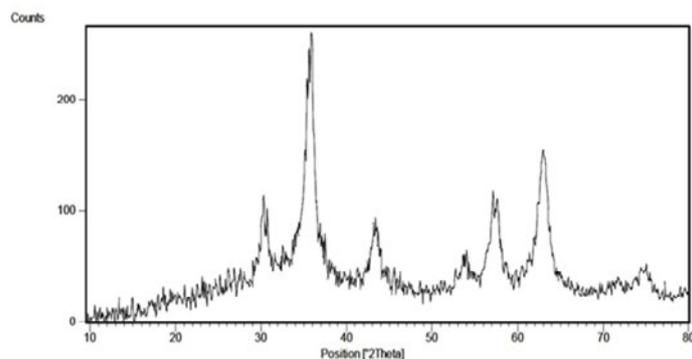
Fig. 3. The XRD pattern of Cross-PAA-SO$_3$H@nano-Fe$_3$O$_4$
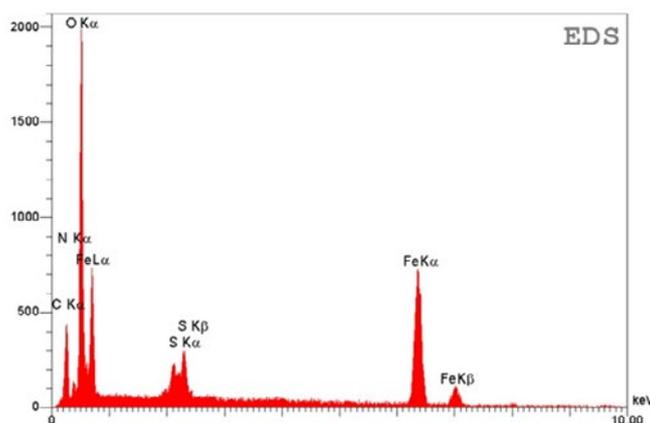
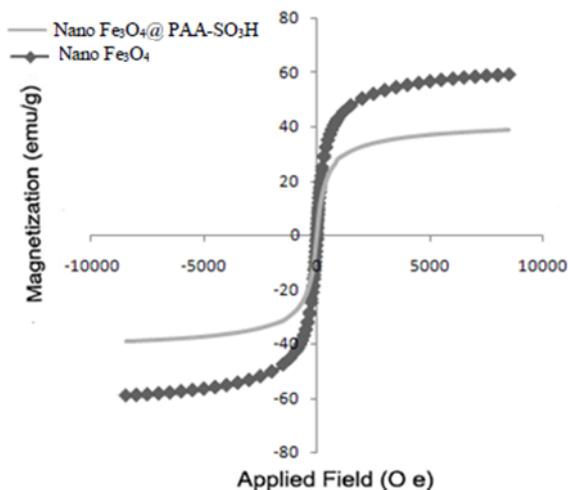Fig. 4. EDS spectrum of Cross-PAA-SO$_3$H@nano-Fe$_3$O$_4$

Fig. 5. The VSM curve of: (a) nano-Fe$_3$O$_4$ and (b) Cross-PAA-SO$_3$H@nano-Fe$_3$O$_4$

reactions were scrutinized using various solvents including EtOH, CH_3CN, water or DMF. The best results were obtained in ethanol and we found that the reaction gave satisfying results by cross-PAA-SO$_3$H@nano-Fe$_3$O$_4$ (7 mg) under

reflux conditions (Tables 2). Scheme 3 shows a proposed mechanism for this reaction in the presence of Cross-PAA-SO$_3$H@nano-Fe$_3$O$_4$ as catalyst. Initially hydrazine hydrate is reacted with 1,-3-dicarbonyl compound to form
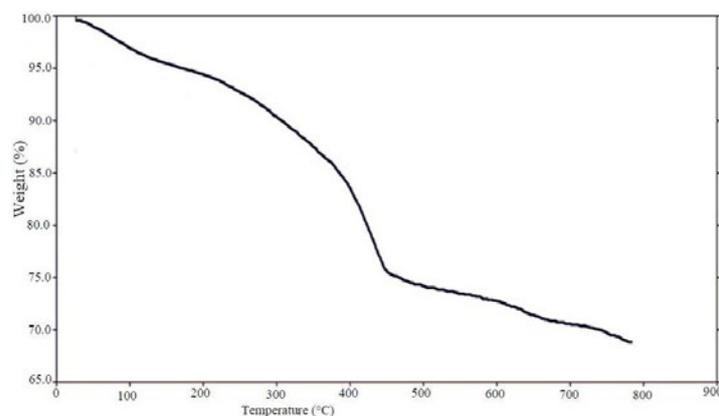

Fig. 6. TGA curve of Cross-PAA-SO$_3$H@nano-Fe$_3$O$_4$.

Table 2. Optimization of reaction conditions using different catalysts [a]

Entry	Solvent (reflux)	Catalyst	Time (min)	Yield (%) [b]
1	EtOH	-------	200	trace
2	EtOH	CAN (5 mol %)	120	17
3	EtOH	NaHSO₄ (10 mol %)	120	32
4	EtOH	Et₃N (10 mol %)	120	38
5	EtOH	Fe₃O₄ NP (50 mg)	120	22
6	EtOH	TsOH (20 mol%)	120	51
7	H₂O	Cross-PAA-SO₃H@nano-Fe₃O₄ (10 mg)	120	45
8	DMF	Cross-PAA-SO₃H@nano-Fe₃O₄ (10 mg)	120	54
9	CH₃CN	Cross-PAA-SO₃H@nano-Fe₃O₄ (10 mg)	120	65
10	EtOH	Cross-PAA-SO₃H@nano-Fe₃O₄ (5 mg)	120	84
11	EtOH	Cross-PAA-SO₃H@nano-Fe₃O₄ (7 mg)	120	88
12	EtOH	Cross-PAA-SO₃H@nano-Fe₃O₄ (10 mg)	120	88
13	EtOH	NiCl₂ (10 mg)	150	42
14	EtOH	ZrOCl₂ (10 mg)	150	58

[a] hydrazine hydrate (1 mmol), 5-chloro-isatin (1 mmol), ethyl acetoacetate (1 mmol), 2-naphthol (1 mmol). [b] Isolated yield
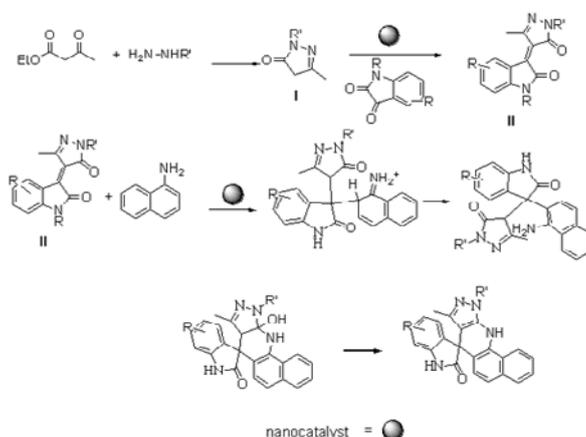
Scheme 3. Proposed reaction pathway for the synthesis of spirooxindoles

Table 3. Synthesis of spirooxindoles

Isatins R	R′	R″	4a or 4b	Product	Time (min)	Yield (%) [a]	M.p. (°C) Found	M.p. (°C) Literature [Ref.]
Cl	H	Me	4a	5a	120	88	196-198	—
H	H	Me	4a	5b	150	86	185-187	—
Me	H	Me	4a	5c	150	83	171-173	—
NO₂	H	Me	4a	5d	120	88	190-192	—
H	Ar	Me	4b	6a	150	82	255-258	255-258 [11]
Cl	Ar	Me	4b	6b	150	84	262-264	264-267 [11]
H	Ar	n-Pr	4b	6c	150	79	300-302	304-307 [11]
Cl	Ar	n-Pr	4b	6d	150	82	295-297	298-301 [11]

[a] Isolated yield

intermediate (I) *via* condensation reaction. Secondly, intermediate (I), in the presence of Cross-PAA-SO₃H@nano-Fe₃O₄, is condensed with isatin derivatives to form intermediate (II) *via* Knoevenagel condensation reaction. In the next step, naphthylamine or 2-naphthol reacts with intermediate (II) through Michael addition. Lastly, the final product is formed by intramolecular cyclization reactions.

We explored the feasibility of the reaction by choosing some representative substrates (Table 3). It has been considered that better yields are achieved with substrates having electron-withdrawing groups. To study the limitation of this catalytic process, hydrazine hydrate or phenylhydrazine, isatins, ketoesters and naphthylamine or 2-naphthol was chosen as substrates. Investigations of the reaction scope revealed that various isatins (bearing electron-withdrawing and electron-donating groups) can be utilized in this protocol (Table 3). The reusability of Cross-PAA-SO₃H@nano-Fe₃O₄ was studied for the reaction of 5-chloro-isatin, hydrazine hydrate, ethyl acetoacetate and 2-naphthol and it was found that product yields decreased to a small extent on each reuse (run 1, 88%; run 2, 88%; run 3, 87%; run 4, 87%; run 5, 86%; run 6, 86%;). After completion of the reaction, the nanocatalyst was easily separated by an external magnet. The catalyst was washed four times with EtOH and dried at room temperature for 20 h.

CONCLUSIONS

In conclusion, we have reported an efficient way for the synthesis of spirooxindoles using Cross-PAA-SO₃H@nano-Fe₃O₄ under reflux condition in ethanol. The method offers several advantages, including high yields, shorter reaction times, reusability of the catalyst and low catalyst loading.

CONFLICT OF INTEREST

The authors declare that there is no conflict of interests regarding the publication of this manuscript.

REFERENCES
1. M. Kitajima, J. Nat. Med., 61, 14 (2007).
2. R. Pandey, S.C. Singh and M.M. Gupta, Phytochem., 67, 2164 (2006).
3. C. Pellegrini, M. Weher, H-J. Borschberg, Helv. Chim. Acta., 79, 151 (1996).
4. G. Bhaskar, Y. Arun, C. Balachandran, C. Saikumar and P.T. Perumal, Eur. J. Med. Chem., 51, 79 (2012).
5. A.H. Abdel-Rahman, E.M. Keshk, M. A. Hanna and S.M. El-Bady, Bioorg. Med. Chem., 12, 2483 (2004).
6. G. Wu, L. Ouyang, J. Liu, S. Zeng, W. Huang, B. Han, F. Wu, G. He and M. Xiang, Mol. Divers, 17, 271 (2013).
7. G. Chen, H.P. He, J. Ding and X.J. Hao, Heterocycl. Commun., 15, 355 (2009).
8. A.S. Girgis, Eur. J. Med. Chem., 44, 1257 (2009).
9. R. Murugan, S. Anbazhagan and S.S. Narayanan, Eur. J. Med. Chem., 44, 3272 (2009).
10. T.L. Pavlovska, R.G. Redkin, V.V. Lipson and D.V. Atamanuk, Mol. Divers 20, 299 (2016).
11. H. Hosseinjani-Pirdehi, K. Rad-Moghadam and L. Youseftabar-Miri, Tetrahedron 70, 1780 (2014).
12. R. Ghahremanzadeh, F. Fereshtehnejad, Z. Yasaei, T. Amanpour and A. Bazgir, J. Heterocycl. Chem., 47, 967 (2010).
13. S. Ahadi, Z. Yasaei and A. Bazgir, J. Heterocycl. Chem., 47, 1090 (2010).

14. M. Mirhosseini Moghaddam, A. Bazgir, M.M. Akhondi and R. Ghahremanzadeh, Chin. J. Chem. 30, 709 (2012).

15. G. Mohammadi Ziarani, A. Badiei, S. Mousavi, N. Lashgari and A. Shahbazi, Chin. J. Catal., 33, 1832 (2012).

16. B. Karmakar, A. Nayak and J. Banerji, Tetrahedron Lett., 53, 5004 (2012).

17. Y. Li, H. Chen, C. Shi, D. Shi and S.J. Ji, Comb. Chem., 12, 231 (2010).

18. M. Shach-Caplan, M. Narkis and M.S. Silverstein, Polym. Adv. Technol., 13, 151 (2002).

19. B. Tamami and S. J. Ghasemi, Mol. Catal. A. Chem., 322, 98 (2010).

20. B. Tamami and S. Ghasemi, Appl. Catal. A. Gen., 393, 242 (2011).

21. M. Rashidi, A.M. Blokhus and A.J. Skauge, Appl. Polym., 119, 3623 (2011).

22. J. Aalaie, E. Vasheghani-Farahani, A. Rahmatpour and M.A. Semsarzadeh, Eur. Polym. J. 44, 2024 (2008).

23. D. Shahabi and H. Tavakol, J. Nanoanalysis., 5, 49 (2018).

24. M. Javdannezhad, M. Gorjizadeh, M. H. Sayahi and S. Sayyahi, J. Nanoanalysis., 5, 287 (2018).